DOI: 10.3901/CJME.2014.1201.174, available online at www.springerlink.com; www.cjmenet.com; www.cjme.com.cn

Dynamic Flow Control Strategies of Vehicle SCR Urea Dosing System

LIN Wei, ZHANG Youtong, and ASIF Malik

Laboratory of Clean Vehicles, Beijing Institute of Technology, Beijing 100081, China

Received April 17, 2014; revised November 20, 2014; accepted December 1, 2014

Abstract: Selective Catalyst Reduction(SCR) Urea Dosing System(UDS) directly affects the system accuracy and the dynamic response performance of a vehicle. However, the UDS dynamic response is hard to keep up with the changes of the engine's operating conditions. That will lead to low NO_X conversion efficiency or NH_3 slip. In order to optimize the injection accuracy and the response speed of the UDS in dynamic conditions, an advanced control strategy based on an air-assisted volumetric UDS is presented. It covers the methods of flow compensation and switching working conditions. The strategy is authenticated on an UDS and tested in different dynamic conditions. The result shows that the control strategy discussed results in higher dynamic accuracy and faster dynamic response speed of UDS. The inject deviation range is improved from being between −8% and 10% to −4% and 2% and became more stable than before, and the dynamic response time was shortened from 200 ms to 150 ms . The ETC cycle result shows that after using the new strategy the NH_3 emission is reduced by 60%, and the NO_X emission remains almost unchanged. The trade-off between NO_X conversion efficiency and NH_3 slip is mitigated. The studied flow compensation and switching working conditions can improve the dynamic performance of the UDS significantly and make the UDS dynamic response keep up with the changes of the engine's operating conditions quickly.

Keywords: select catalyst reduction(SCR), urea dosing system(UDS), dynamic flow, control strategies

1 Introduction

To meet the emission regulations of European Ⅳ and European Ⅴ , High-pressure Common Rail(HCR) and Selective Catalyst Reduction(SCR) are used to reduce PM and NO_X in diesel engine as the mainstream technologies[1–4].

The injection rate algorithms and Urea Dosing System(UDS) flow control strategy are focused in studies on vehicle Urea Water Solution(UWS) injection. The performance of UDS directly affects the matching of SCR diesel engine. The aim of UDS control strategy is to make the actual injection rate more and more closer to the theoretical value, especially in the dynamic conditions. At present, almost 99% of the diesel vehicles work in dynamic operating conditions. So their NO_X emission is a dynamic process. Therefore, excellent dynamic performance is the essential characteristics of the SCR system integrated on the engine. When the actual injection rate is lower than the theoretical value, the NO_X can't be completely reduced. Whereas, if the actual injection rate is higher than the theoretical value, NH_3 can't be completely oxidized and resultantly generates secondary pollution[5–7]. BONFILS A, et al[8], proposed a control strategy for an automotive SCR system with a NO_X sensor in a feedback loop. The result of experiment, which was obtained calibration method, illustrated the relevance and performance of the proposed approach. MARK S, et al[9], finished some experimental studies of different SCR control strategies. The result showed that closed-loop feedback control model with an embedded NH_3 sensor could significantly improve the NO_X conversion efficiency and reduce NH_3 emission. In such situation, SCR catalyst could be reduced by 22% in volume. Some simulations of SCR system were finished. YORK A P and VAN H R, et al[10–11], developed a one dimensional software to analyze the influence of the NO and NO_2 ratio on the NO_X conversion efficiency. CHI J N, et al[12], and WURZENBERGER J C, et al [13], finished some SCR system control simulations by the use of Boost and Matlab Simulink. TAN J [14], ZHANG R J[15], TONG D H[16], LIU J, et al [17], studied the control strategies with different methods. WANG L L[18] did some simulation of UWS injection control based on a non-air-assisted UDS, developed an urea nozzles peak-hold circuit with the circuit characteristics of the analog operational amplifier, designed an urea pressure fuzzy PID control algorithm, and optimized the method of UWS pressure stabilizing. The dynamic characteristics of SCR system were closely associated to UDS performance, especially to the dynamic response speed and the dynamic injection accuracy.

This paper presents the dynamic flow control of an air-assisted volumetric UDS, analyzes its working theory and subsequently explained the UWS injection process by with mathematical theory. Finally, a method of dynamic flow compensation was established based on each work

* Corresponding author. E-mail: lin_wei_sky@163.com
Supported by National Hi-tech Research and Development Program of China(863 Program, Grant No. 2012AA111708)

cycle characteristics of the air-assisted volumetric UDS by dividing it into four different working conditions. When the dynamic response speed of the UDS was optimized by the method of conditions switching, the dynamic injection accuracy remained in the original scope.

2 Mathematical Analysis

2.1 Measurement principle

UDS measures the volumetric UWS accurately. Work cycle of the UDS consists of two adjacent processes i.e. suction and injection, as shown in Fig. 1. The theoretical UWS flow rate through the UDS is q, and the flow rate is $q(t)$ at time t(t is between t_0 and t_2), as

$$q(t)=\begin{cases} q(t_0^+)+\int_{t_0^+}^{t} a(t)\mathrm{d}t, & t\in(t_0,t_1), \\ q(t_1^+)+\int_{t_0^+}^{t} a(t)\mathrm{d}t, & t\in(t_1,t_2), \end{cases} \tag{1}$$

where $a(t)$ is the acceleration of the UWS. Connecting position of the two processes(suction and injection) is called “change point”, where the flow rates are the same value in the opposite direction, as

$$\begin{cases} q(t_0^-)=-q(t_0^+)=\left|q(t_0^+)\right|, \\ q(t_1^+)=-q(t_1^-)=\left|q(t_1^-)\right|, \\ q(t_2^-)=-q(t_2^+)=\left|q(t_2^+)\right|. \end{cases} \tag{2}$$

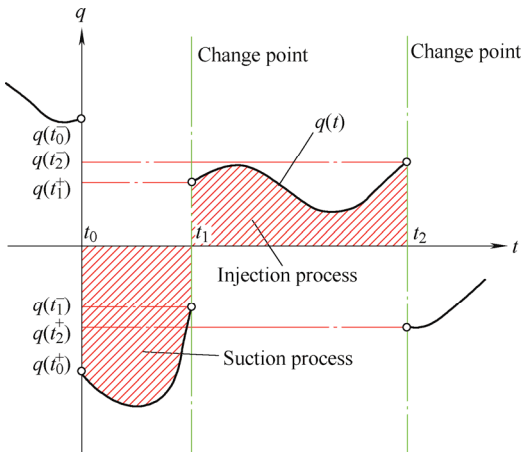

Fig. 1. Theoretical flow rate variation in each working cycle of the UDS

In Fig. 1 t_0, t_1, t_2 are all “change point”. According to Eq. (2), Eq. (1) can be modified as

$$q(t)=\begin{cases} q(t_0^+)+\int_{t_0^+}^{t} a(t)\mathrm{d}t, & t\in(t_0,t_1), \\ \left|q(t_0^+)+\int_{t_0^+}^{t_1^-} a(t)\mathrm{d}t\right|+\int_{t_0^+}^{t} a(t)\mathrm{d}t, & t\in(t_1,t_2). \end{cases} \tag{3}$$

Based on the features of the air-assisted volumetric UDS, Eq. (4) can be obtained. The designed maximum working volume is Q, thus Q is the UWS volume in suction process or injection process in each UDS working cycle, as Eq. (5):

$$\int_{t_0^+}^{t_2^-} q(t)\mathrm{d}t=0, \quad t\in(t_0,t_1)\cup(t_1,t_2), \tag{4}$$

$$\left|\int_{t_0^+}^{t_1^-} q(t)\mathrm{d}t\right|=\int_{t_1^+}^{t_2^-} q(t)\mathrm{d}t=Q, \quad t\in(t_0,t_1)\cup(t_1,t_2). \tag{5}$$

2.2 Dynamic flow compensation

The aim of dynamic flow compensation is to inject the required UWS in suction process as soon as possible. After the dynamic flow compensation is finished, UDS measures and injects UWS as required in injection process. The required dynamic injection rate varies with the time, as shown in Fig. 2. The total demand of UWS in each UDS working cycle is Q_d, and because Q is the max volume flow rate of the UDS in each injection process, Q_d can be calculated as

$$Q_\mathrm{d}=\int_{t_0}^{t_2^-} q_\mathrm{d}(t)\mathrm{d}t=Q, \tag{6}$$

where q_d is the demand UWS injection rate.

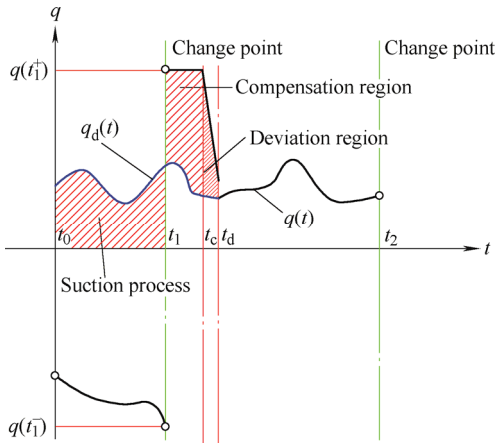

Fig. 2. Dynamic flow compensation in each working cycle of the UDS

Practically, suction process is between t_0 and t_1. During this process, the required UWS is not injected out of the UDS, which has to be compensated between t_1 and t_2 in the next process. The total amount of the UWS needed to be compensated is Q_c, which can be calculated as

$$Q_\mathrm{c}=\int_{t_0}^{t_1} q_\mathrm{d}(t)\mathrm{d}t, \tag{7}$$

where the flow compensation is initiated at t_1 and finished

at t_c. Therefore, the flow compensation duration T_c can be calculated as

$$T_c = t_c - t_1, \quad t_c \in [t_1, t_2). \tag{8}$$

Some UWS is required in the period between t_1 and t_c, so the compensation process should be finished as soon as possible for accelerating the dynamic response speed of the UDS. During this time, the UDS should work at its maximum capability, as

$$Q_c = \int_{t_0}^{t_1} q_d(t)\mathrm{d}t = \int_{t_1}^{t_c} [q(t) - q_d(t)]\mathrm{d}t. \tag{9}$$

To get the minimum T_c in this process, the maximum value of $q(t)$ is requires, as

$$q(t) \equiv q_{max} \quad t \in (t_1, t_c), \tag{10}$$

after putting into Eq. (9),

$$Q_c = \int_{t_1}^{t_c} [q_{max} - q_d(t)]\mathrm{d}t = q_{max}(t_c - t_1) - \int_{t_1}^{t_c} q_d(t)\mathrm{d}t, \tag{11}$$

through Eq. (7) and Eq. (11), t_c can be calculated as

$$t_c = \frac{\int_{t_0}^{t_c} q_d(t)\mathrm{d}t}{q_{max}} + t_1. \tag{12}$$

After the flow compensation is finished at time t_c, UDS will immediately perform a speed variation and inject UWS according to the variation of q_d. Because q is synchronized with q_d at time t_c, the injection deviation of the UDS between t_d and t_c can be calculated as

$$\Delta Q = \int_{t_c}^{t_d} [q(t) - q_d(t)]\mathrm{d}t, \tag{13}$$

where

$$q(t) = q_{max} + \int_{t_c}^{t} a(t)\mathrm{d}t, \tag{14}$$

while q is synchronized with q_d at time t_c,

$$q(t_d) = q_{max} + \int_{t_c}^{t_d} a(t)\mathrm{d}t = q_d(t_d). \tag{15}$$

By via Eq. (15) and Eq. (14), Eq. (13) can be written as

$$\Delta Q = \int_{t_c}^{t_d} [q_{max} + \int_{t_c}^{t} a(t)\mathrm{d}t - q_d(t)]\mathrm{d}t = q_{max}(t_d - t_c) - \int_{t_c}^{t_d} q_d(t)\mathrm{d}t + \int_{t_c}^{t_d}\int_{t_c}^{t} a(t)\mathrm{d}t\mathrm{d}t. \tag{16}$$

Thus, minimum ΔQ can be obtained when

$$a(t) \equiv a_{min} \quad t \in (t_c, t_d). \tag{17}$$

Furthermore, with $|a_{min}|=a_{max}$, ΔQ_{min} can be calculated as

$$\Delta Q_{min} = (q_{max} - a_{min}t_c)(t_d - t_c) + \frac{1}{2}a_{min}(t_d^2 - t_c^2) - \int_{t_c}^{t_d} q_d(t)\mathrm{d}t, \tag{18}$$

where $t_d = [q_d(t_d) - p_{max}]/a_{min} + t_c$.

2.3 Dynamic conditions switching

Each working cycle of the UDS is divided into four conditions for independent analyzing, from which the dynamic response speed and injection deviation can be optimized, as shown in Fig. 3.

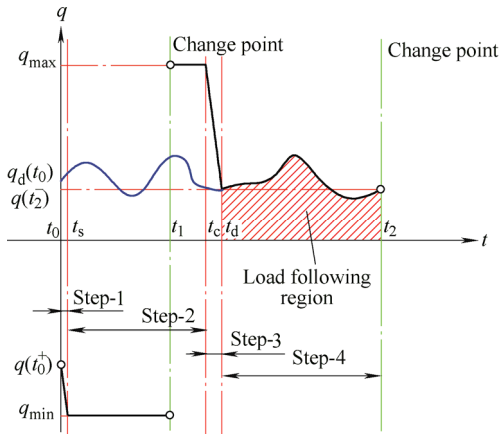

Fig. 3. Dynamic conditions switching in each working cycle of the UDS

Step-1: Emergency accelerating region is between t_0 and t_s. The purpose of this step is to reduce the suction process time as short as possible. In other words, it is for reducing q to q_{min} as quickly as possible. During Step-1, $q(t)$ can be calculated as

$$q(t) = q(t_0^+) + \int_{t_0}^{t} a(t)\mathrm{d}t \quad t \in (t_0, t_s], \tag{19}$$

q is reduced to q_{min} in time t_s, so

$$q(t_s) = q(t_0^+) + \int_{t_0}^{t_s} a(t)\mathrm{d}t = q_{min}, \tag{20}$$

to achieve the minimum T_{s1} (T_{s1min}), the condition is

$$a(t) \equiv a_{min}, \quad t \in (t_0, t_s), \tag{21}$$

and T_{s1min} can be calculated as

$$T_{s1min} = \frac{q_{min} - q(t_0^+)}{a_{min}}, \tag{22}$$

where $|a_{min}|=a_{max}$, T_{s1} is the period of Step-1.

Step-2: Full load region is between t_s and t_c. The purpose of this step is to reduce the suction process time and compensate the flow as soon as possible. At t_1 time, the rate and acceleration of the flow is inverted. UDS speed does not required to be changed and continues to operate at full load as

$$\begin{cases} |q(t)| \equiv q_{max}, \\ a(t) \equiv 0, \end{cases} \quad t \in (t_s, t_1) \cup (t_1, t_c], \tag{23}$$

from Eq. (5) and Eq. (12), T_{s2} can be calculated as

$$T_{s2} = \frac{Q - \left|\frac{1}{2}(t_s - t_0)[q_{min} + q(t_0^+)]\right|}{|q_{min}|} + \frac{\int_{t_0}^{t_c} q_d(t)\mathrm{d}t}{q_{max}} = \frac{Q - \left|\frac{1}{2}(t_s - t_0)[q_{min} + q(t_0^+)]\right| + \int_{t_0}^{t_c} q_d(t)\mathrm{d}t}{q_{max}}, \tag{24}$$

where T_{s2} is the period of Step-2, and $T_{s2}=(t_1-t_s)+(t_c-t_1)$, through Eq. (22) and Eq. (24):

$$T_{s2} = \frac{Q - \left|\frac{1}{2a_{min}}[q_{min}^2 - q^2(t_0^+)]\right| + \int_{t_0}^{t_c} q_d(t)\mathrm{d}t}{q_{max}}. \tag{25}$$

Step-3: Fast approximation region is between t_c and t_d. The purpose of this step is to achieve actual injection rate which is approximately equivalent to the required value as fast as possible. In this situation, the injection deviation can be reduced to the minimum value. The UDS will quickly vary its speed to the required value at t_d time. During Step-3, $a(t)$ and $q(t)$ can be calculated as

$$\begin{cases} a(t) \equiv a_{min}, \\ q(t) = q_{max} + a_{min}(t - t_c), \end{cases} \quad t \in (t_c, t_d], \tag{26}$$

from Eq. (15) and Eq. (17), T_{s3min} can be calculated as

$$T_{s3min} = \frac{q_d(t_d) - q_{max}}{a_{min}}. \tag{27}$$

where T_{s3} is the period of Step-3, and $T_{s3}=(t_d - t_c)$.

Step-4: Load following region is between t_d and t_2. The purpose of this step is to make the injection rate as close to the required value as possible. Theoretically, the curves of $q(t)$ and $q_d(t)$ in this region is completely overlapped. In other words, the relationship of $q(t)$ and $q_d(t)$ in this region can be expressed as

$$q(t) \equiv q_d(t), \quad t \in (t_d, t_2]. \tag{28}$$

3 Experiments and Results

The dynamic injetion accuracy and dynamic response speed of the UDS, which were usually reflected by comparing the actual injection rate and theorical value, had been verified in the experiments. And the characteristics of the UDS with and without using the said strategy were also compared. Actually, it was difficult to measure the dynamic injection rate, therefore, the drive signal frequency of the motor was choosen to verify the gap between the actual and the required injection rates. The injection rate of the UDS in this experiment was changed exactlly with its step motor and could be calculated as

$$q_a = \frac{2Q \times F_m \times \theta}{\lambda \times 360}, \tag{29}$$

where q_a is the actual injection rate, Q is the maximum flow volume of the UDS in each injection process, F_m is the actual drive signal frequency of the motor, λ is the gear ratio of the motor and UDS, and θ is the step angle of the motor. With the use of the electronic balancing scale, the injection accuracy of the UDS can be calculated by the changes of the UWS quality in the mesuring glasses befor and after the injection, and the trends of q_d and F_m will be send to the monitoring interface on the computer by CAN bus, as illustrated in Fig. 4.

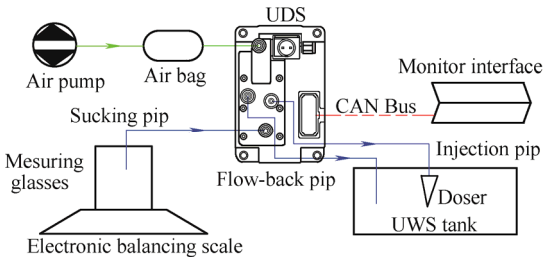

Fig. 4. UDS experiment platform block diagram

In order to compare the diesel engine emission data before and after using the strategy studied in this paper, an engine experiment platform had been established, as shown in Fig. 5. The specifications of main equipment in the engine experiment platform are listed in Table 1.

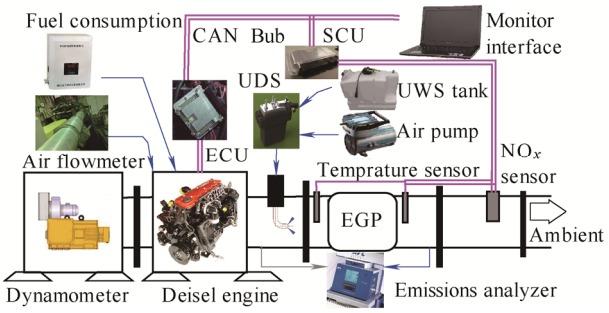

Fig. 5.　Engine experiment platform block diagram

Table 1.　Specifications of main equipment

Name	Type	Manufacturer	Remark
Dynamometer	GWD300	POWERLINK	Eddy current style
Fuel consumption	FC2210	POWERLINK	Quality style
Air flow meter	ToCeil	Shanghai ToCeil Engine Testing Equipment	Hot film style
Emissions analyzer	SESAM4.0	AVL	Fourier transform infrared spectroscopy

3.1　Control process validation

In order to validate the flow compensation process and the condition switching process, q_d =0.5 g/s was set and the trends of F_m in the start-up phase was displayed on the monitor screen, as shown in Fig. 6. Point 1 is a power-on reset process. The motor of the UDS accelerated to maximum rate quickly, and then stopped immediately on the UDS reset point. Point 2 is a start-injection process. After receiving the UWS injection command, the UDS started up quickly. In the first time, the UDS finished its suction process before the motor reached maximum speed. And the motor speed dropped to the current required injection rate quickly. Point 3 is normal-injection process. After the normal UDS injection, when the suck phase came, the flow compensation and condition switching wre performed. In this time, F_m curve showed peaks periodically. And then it dropped to the required injection rate quickly.

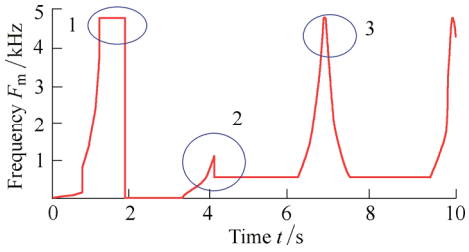

Fig. 6.　Start-up phase (q_d=500 mg/s)

Zooming in point 3, as shown in Fig. 7, the switching of four conditions can be distinguished clearly. Flow compensation occurred at Step-2 which is named “full load region”. And Step-2 was completed in a very short time.

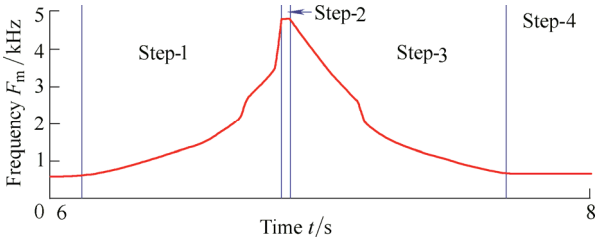

Fig. 7.　Conditions switching process

In order to identify whether the new dynamic strategy has an impact on the steady-state performance of the UDS or not, the steady-state accuracy of the system is required to be varified. Thus, the steady-state accuracy of the UDS was compared before and after using the new strategy. The outcomes are shown in Fig. 8.

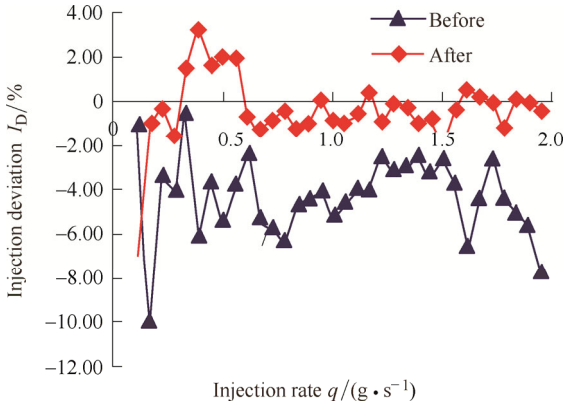

Fig. 8.　Steady-state accuracy (before and after using the new strategy studied in this paper)

(1) With the use of new strategy, when the injection rate is below 0.3 g/s, the deviation is significant.

(2) When the injection rate is between 0.3 g/s and 2 g/s, the UDS after applying the new strategy steady-state accuracy is improved a lot. The deviation range is changed from being between –8% and 0% to –2% and 4%.

(3) After applying the new strategy, the deviation curve becomes more stable than before.

The comparison proved that the new strategy made the UDS more stable and significantly improved its steady-state accuracy.

3.2　Dynamic response speed validation

To validate dynamic response speed, the trends of F_m and q_d were compared. Providing that the total injection time was 180 s, the UDS was tested in dynamic conditions. The results are shown in Table 2, where variation form is the variation of the required injection rate, q_{dmax} is the max injection rate, q_{dmin} is the min injection rate, Δt is the period of the injection rate chenged, and T_D is the total dosing time.

Table 2.　UDS dynamic conditions (change Δt)

Variation form	Max injection rate q_{dmax}/(mg • s^{-1})	Min injection rate q_{dmin}/(mg • s^{-1})	Period of the rate changes Δt/ms	Total injection time T_D/s
Sine	2000	0	100/150/200	180
Random	2000	0	100/150/200	180

The dynamic conditions were set as Table 2. Thus six group q_d curves were obtained as shown in Fig. 9.

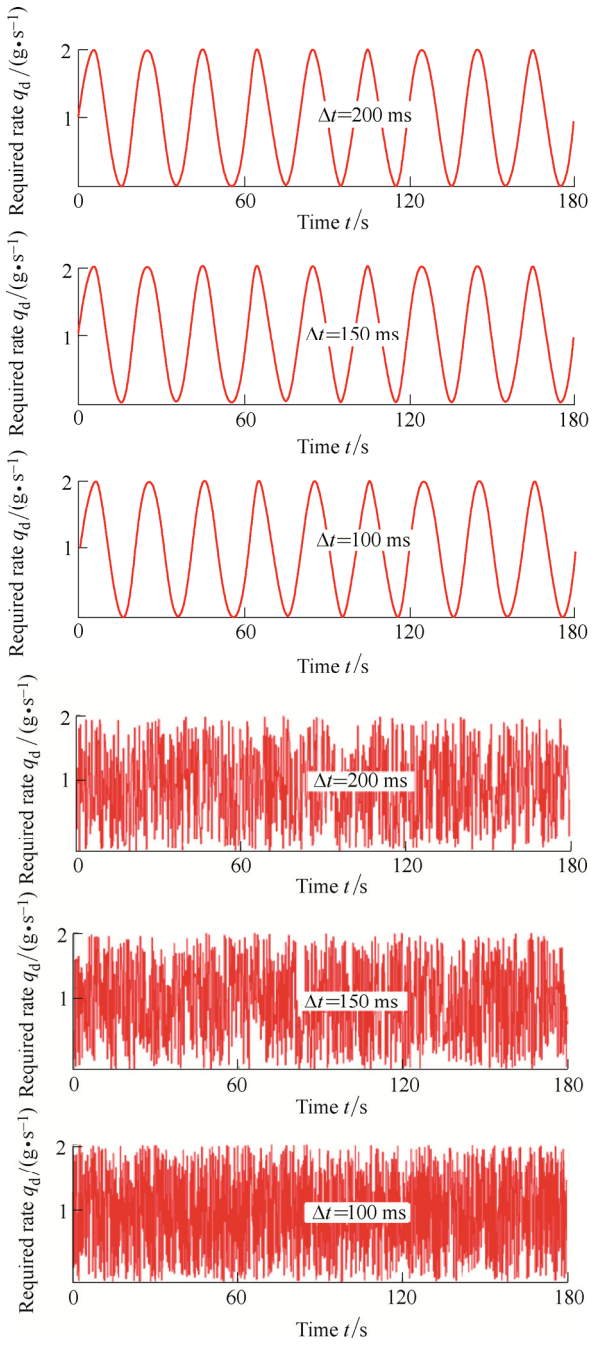

Fig. 9. Required dynamic injection rate (T_D=180 s, Δt changes)

F_m curve and q_d curve were generated on the monitoring interface after the test. And to perform detail analysis, a part of the valid data, with Δt=200 ms, were selected, amplified and curved, as shown in Fig. 10.

(1) When q_d was varied in sinusoidal form, F_m followed the pace of q_d strictly as fluctuating in sinusoidal form.

(2) In the sine condition, peaks of the F_m curve mainly gathered in the area of high injection rate. That was because in this case the suction process appeared in high frequency. The UDS condition was changed continuously. And Step-1, Step-2, and Step-3 as shown in Fig. 3 were completed quickly in 200 ms. That was why there were a lot of peaks in the F_m curve.

(3) In the sine condition, F_m curve is smooth in the region of low injection rate. That was because in this case the injection process was not completed, and F_m changed exactly with q_d as indicated in Step-4 shown of Fig. 3.

(4) In the random condition, the injection rates of two adjacent injections fluctuated widely. However, almost all of the samples showed that the scope and the pace of F_m change firmly with those of q_d.

(5) In the random condition, there was a peak in the circled location where the trends of F_m and q_d were not similar. That's because the UDS was in suction process.

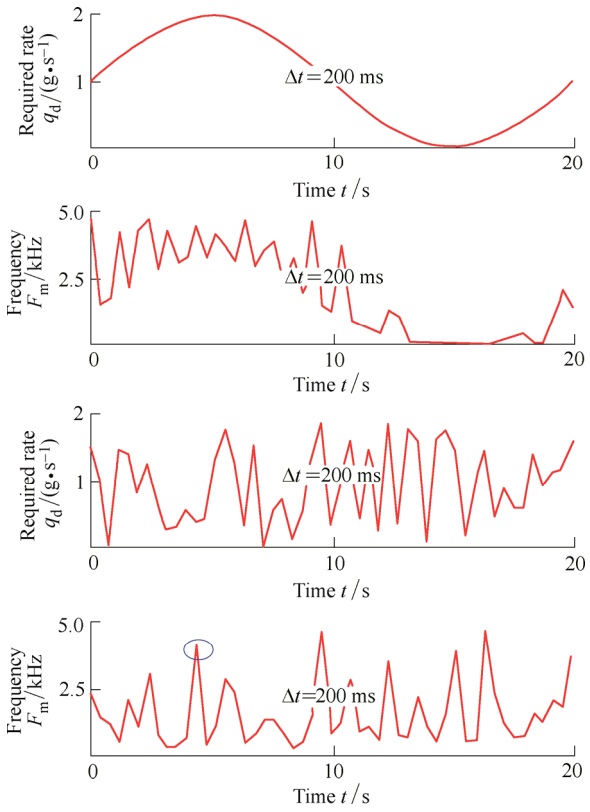

Fig. 10. Trends of F_m and q in dynamic conditions (T_D=180 s, Δt=200 ms)

The analyses above show that F_m can response quickly to keep up with the pace of q_d in the case of Δt=200 ms. Other dynamic conditions were also analyzed in the same way, as depicted in Fig. 11.

(1) In the two sinusoidal conditions, F_m firmly followed the pace of q_d. And peaks of the F_m curve largely clustered in the area of high injection rate.

(2) In the two sinusoidal conditions, the shorter the Δt was, the denser the peaks of the F_m curve were. Due to the more frequent changes of the injection rate, the steps of the motor get disorganized.

(3) In the random condition, ignoring the suction process, F_m follow the pace of q_d in the case of Δt=150 ms.

(4) In the random condition, overlooking the suction process, F_m follow the pace of q_d in the case of Δt=100 ms. In some parts of the high-frequency region, low amplitude compression response (hysteresis response) was noticed, as identified in the circled locations of Fig. 11.

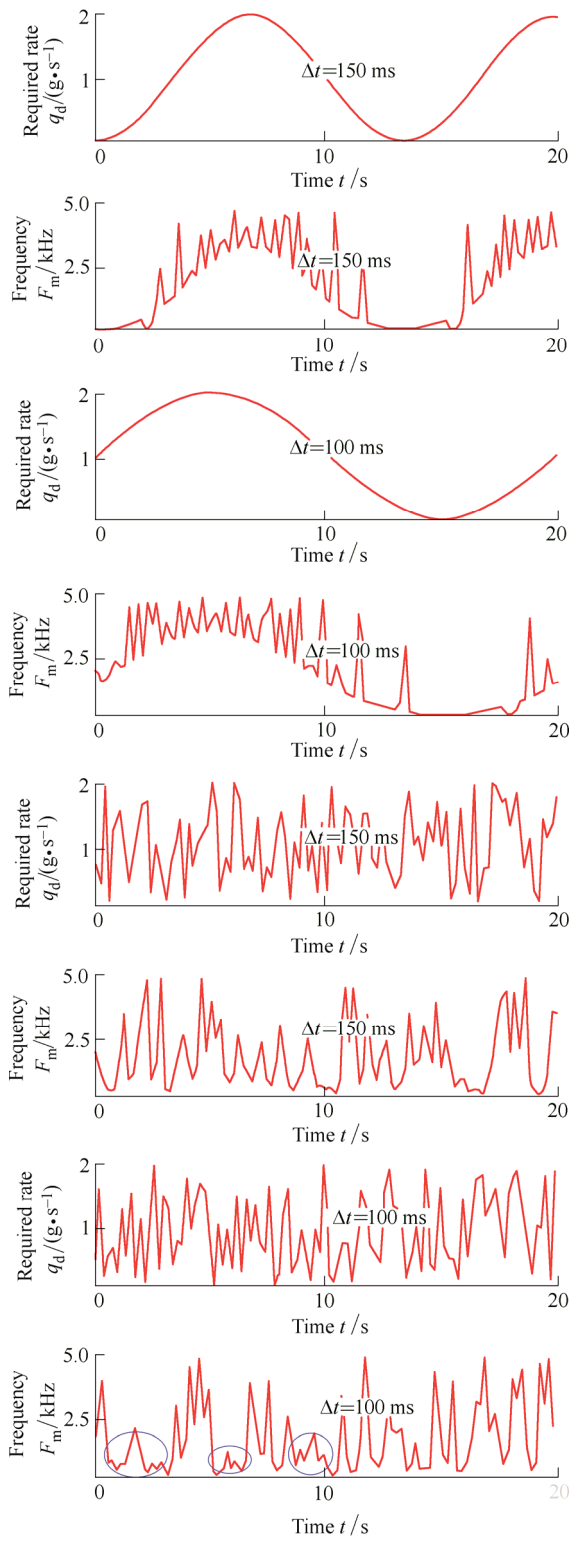

Fig. 11.　Trends of F_m and q_d in dynamic conditions (T_D=180 s, Δt changed)

The result shows that F_m can response quickly in the case of Δt=150 ms. When Δt=100 ms, F_m will be disorganized in sinusoidal conditions. And hysteresis response in random conditions will appear.

3.3　Dynamic injection accuracy divergence

In order to compare the dynamic accuracies of the UDS before and after using the new strategy, the UDS was tested in dynamic conditions as shown in Table 3. With the dynamic conditions set as shown in Table 3, six group of q_d curves were obtained, as pictured in Fig. 12. Three of them were in the form of Sine, while others were Random.

Table 3.　UDS dynamic conditions (change T_D)

Variation form	Max injection rate q_{dmax}/(g • s^{-1})	Min injection rate q_{dmin}/(g • s^{-1})	Period of rate changes Δt/ms	Total injection time T_D/s
Sine	2	0	200	60/120/180
Random	2	0	200	60/120/180

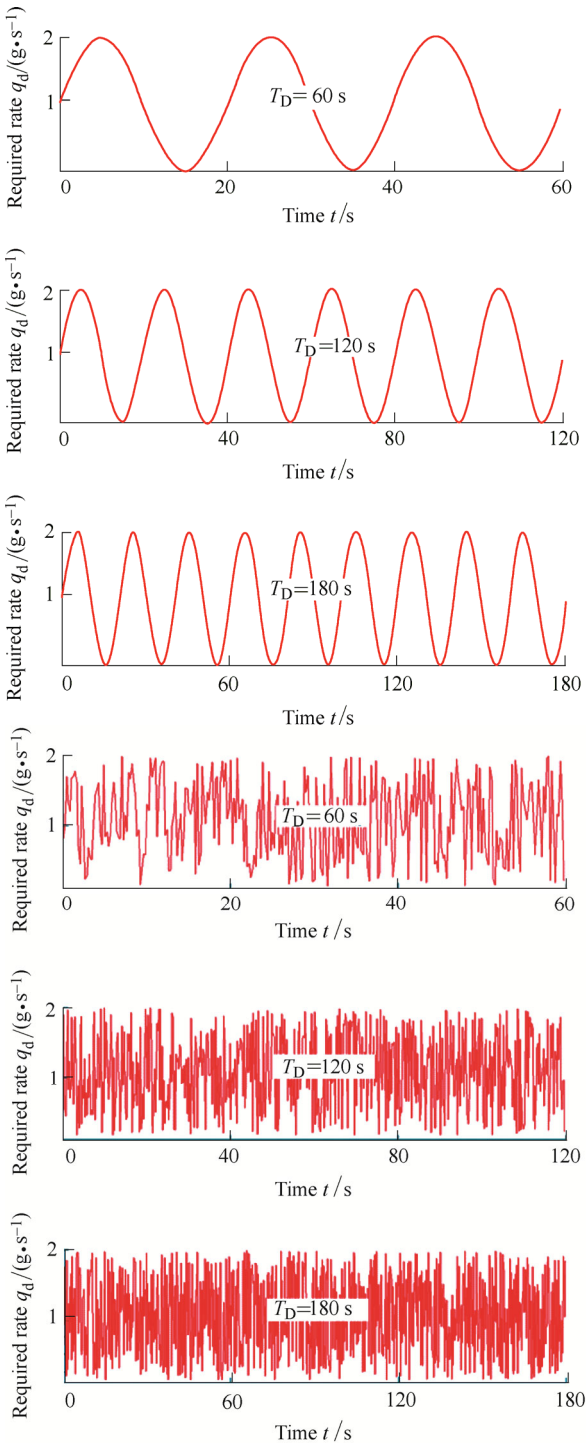

Fig. 12.　Required dynamic injection rate (Δt=200 ms, T_D changes)

In order to reduce test deviation, each conditon had been tested for three times. The results are illustrated in Fig. 13.

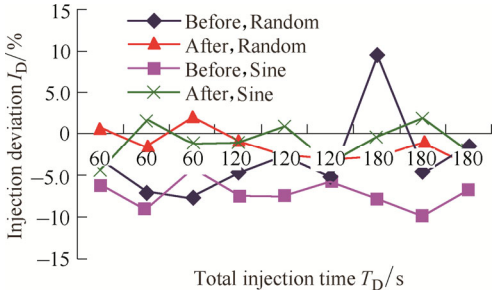

Fig. 13. Dynamic accuracy (before and after using the new strategy studied in this paper, Δt=200 ms, change T_D)

(1) In the random conditions, after using the new strategy the dynamic accuracy of the UDS was improved. The deviation range was changed from being between –8% and 10% to –4% and 2% and became more stable than before.

(2) In the sine conditions, with the use of the new strategy, the dynamic accuracy of UDS was improved siginificently. The deviation range was changed from being between –10% and –4% to –4% and 2%.

This indicates that the new strategy tends the UDS towards more stable in dynamic conditions. And it obviously enhanced its dynamic accuracy.

The UDS after using the new strategy was tested in dynamic conditions as shown in Table 2. On Setting T_D=180 s and changing Δt, the results are gotten as shown in Fig. 14.

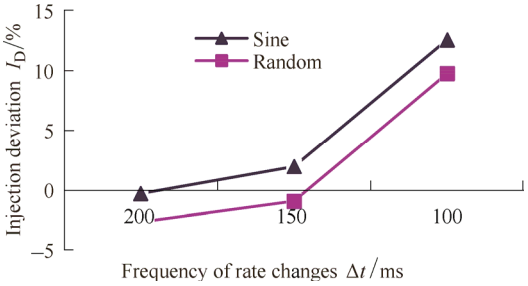

Fig. 14. Dynamic accuracy(after using the new strategy studied in this paper, change Δt, T_D=180 s)

(1) Wether in random conditions or sine conditions, the injection deviation was increased with the decreasing of Δt.

(2) In the case of Δt=200 or 150 ms, the deviation was between –3% and 2%. In the case of Δt=100, the deviation was between –10% and 14%.

This shows that with the use of new strategy the UDS has a good injection accuracy in the case of Δt=200 or 150 ms but not in the case of Δt=100 ms.

3.4 ETC cycle result

The comparison of the emission data on diesel engine in ETC cycle before and after using the strategy of the UDS is shown in Fig. 15.

The result indicates a considerably high efficiency of NO_X conversion in each of the two tests. After using the new strategy, the NH_3 slip was also reduced 60%, and the emission level of engine's NO_x and NH_3 were improved from European Ⅳ to European Ⅴ standard.

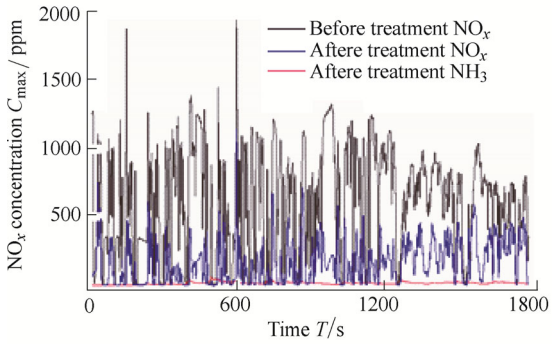

(a) Without new strategy:NO_x 2.09 g/(kW·h), NH_3 16 ppm

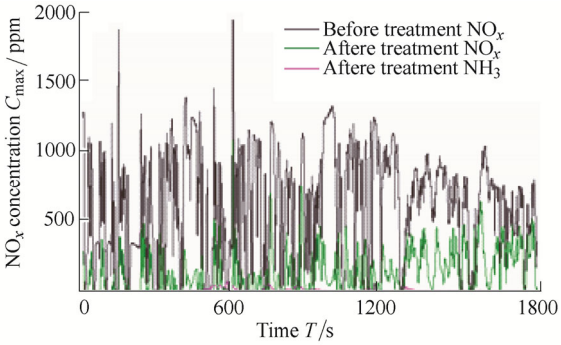

(b) Using new strategy:NO_x 2.0 g/(kW·h), NH_3 10 ppm

Fig. 15. Engine ETC cycle emission results

4 Conclusions

(1) The dynamic injection accuracy and the dynamic response speed are optimized by the method of dynamic flow compensation and dynamic conditions switching, and it make the UDS to achieve highly stable injection accuracy.

(2) When the dynamic response speed is kept constant (Δt=200 ms), after using the new strategy the UDS has more excellent injection accuracy both in dynamic conditions and steady-state conditions.

(3) On accelerating the response speed (Δt=150 ms), the motor can response quickly to keep up with the pace of the injection rate, and the injection deviation is about 2% which can be ignored. The strategy is proved as capable of improving the response speed of the UDS.

(4) Accelerating the response speed in excess (Δt=100 ms) will make the motor to be disorganized, and the injection accuracy will be deteriorated sharply.

(5) The results of ETC cycle test show that after using the new strategy the NH_3 emission is reduced 60% , the NO_X emission remains almost unchanged, and the UDS has a more superior performance. The issue that the UDS response performance can't keep up with the changes of the engine's operating conditions can be resolved. And NH_3 emission can be reduced along with the reduction of NO_X emission.

References

[1] JOHNSON T V. Diesel emission control in review[J]. *SAE Paper*, 2009, 0121(01).

[2] JOHNSON T V. Review of diesel emissions and control[J]. *SAE Paper*, 2010, 0301(01).

[3] JOHNSON T V. Diesel emissions in review[J]. *SAE Paper*, 2011, 0304(01).

[4] CLOUDT R, BAERT R, WILLEMS F, et al. SCR-only concept for heavy-duty euro VI applications[J]. *MTZ*, 2009, 70(9): 58–63.

[5] SEHER D H E, REICHELT M, WICKERT S. Control strategy for NO_X emission reduction with SCR[J]. *SAE Paper*, 2003, 3362(01).

[6] KAMMERSTETTER H, WERNER M, DOELL R, et al. The challenge of precise characterizing the specific large-span flows in urea dosing systems for NO_X reduction[J]. *SAE Paper*, 2008, 1028(01).

[7] KASS M D, THOMAS J F, LEWIS S A, et al. Selective catalytic reduction of NO_X emissions from a 5.9 liter diesel engine using ethanol as a reductant[J]. *SAE Paper*, 2003, 3244(01).

[8] BONFILS A, CREFF Y. Closed-loop control of a SCR system using a NO_X sensor cross-sensitive to NH_3[J]. *Journal of Process Control*, 2013, 1649(1): 1–11.

[9] MARK S, JOHN N. Monitoring, feedback and control of urea SCR dosing systems for NO_X reduction: Utilizing an embedded model and ammonia sensing [J]. *SAE Paper*, 2008, 1325(01).

[10] YORK A P E, WATLING T C, COX J P, et al. Modeling an ammonia SCR $DeNO_X$ catalyst-model development and validation[J]. *SAE Paper*, 2004, 0155(01).

[11] VAN H R, VERBEEK R, WILLEMS F, et al. Optimization of Urea SCR $DeNO_X$ system for HD diesel engines[J]. *SAE Paper*, 2004, 0154(01).

[12] CHI J N, DACOSTA H F M. Modeling and control of a Urea-SCR after treatment system[J]. *SAE Paper*, 2005, 0966(01).

[13] WURZENBERGER J C, WANKER R. Multi-Scale SCR modeling, 1D kinetic analysis and 3D system simulation[J]. *SAE Paper*, 2005, 0948(01).

[14] TAN J. The study of strategy for a SCR system to reduce NO_X emission from a heavy duty diesel engine[D]. *Wuhan*: *Wuhan University of Technology*, 2007. (in Chinese)

[15] ZHANG J R. Study on urea dosing strategy of SCR for heavy duty diesel engine[D]. *Jilin: Jilin University*, 2011. (in Chinese)

[16] TONG D H. Study on control strategy of SCR technology to reduce NO_X emission from heavy-duty diesel engine[D]. *Jinan: Shandong University*, 2009. (in Chinese)

[17] LIU J, WU S K, HE G G. et al. Study of strategy for a SCR system[J]. *Tractor& Farm Transporter*, 2010, 37(3): 34–36. (in Chinese)

[18] WANG L L. Development of control technology of non-air assisted urea-SCR injection system for diesel engine[D]. *Jilin: Jilin University*, 2012. (in Chinese).

Biographical notes

LIN Wei, born in 1987, is currently a PhD candidate at *Beijing Institute of Technology, China*. He received his master degree from *Beijing Institute of Technology, China*, in 2012. His research interests include SCR system control.
Tel: +86-18610633418; E-mail: lin_wei_sky@163.com

ZHANG Youtong, born in 1965, is currently a professor and a doctoral instructor at *Beijing Institute of Technology, China*. He received his PhD degree from *Beijing Institute of Technology, China*, in 1995. His research interests include vehicle power system control.
E-mail: youtong@bit.edu.cn

ASIF Malik, born 1985, is a master candidate at *Beijing Institute of Technology, China.* He received his bachelor of engineering (BE) degree from *National University of Sciences and Technology, Pakistan*, in 2006. Since then he has been serving as a manager in an armored vehicles manufacturing organization of his country. His research is aimed to engine performance analysis especially the exhaust emission control with SCR.